Three-dimensional Hydrogels of Alginate/chitosan Semi-interpenetrating Polymer Networks and Nanocelluloses

Priscila Siqueira
Universidade Federal de Ouro Preto Instituto de Ciencias Exatas e Biologicas
Ana de Lima
Universidade Federal de Minas Gerais
Felipe Medeiros
Universidade Federal de Minas Gerais
Augusta Isaac
Universidade Federal de Minas Gerais
Katia Novack
Universidade Federal de Ouro Preto Instituto de Ciencias Exatas e Biologicas
Vagner Botaro
UFSCar: Universidade Federal de Sao Carlos
Eder Siqueira (eder_siqueira@ymail.com)
Universidade Federal de Minas Gerais Instituto de Ciencias Exatas https://orcid.org/0000-0003-3147-7103

Research Article

Keywords: hydrogels, alginate, chitosan, nanocelluloses, biocompatibility

Posted Date: October 18th, 2021

DOI: https://doi.org/10.21203/rs.3.rs-706130/v1

Abstract

The hydrogels are advanced materials used in biomedical applications during wound healing, controlled drug release and to prepare scaffolds. In this work are prepared hydrogels of alginate/chitosan (*Alg/Ch*) semi-interpenetrating polymer networks (semi-IPN's) and nanocelluloses. The hydrogels after preparation by freeze drying are namely simply as gels. The cellulose nanocrystals (CNC's) are obtained from acid hydrolysis of bleached *Eucalyptus* pulps and oxidized cellulose nanocrystals (CNCT's) prepared by (2,2,6,6-tetramethylpiperidin-1-yl)oxyl radical catalyzed reaction as known as TEMPO reaction. The cellulose nanofibers (NFC's) are obtained from mechanical shearing of cellulose pulps and oxidized NFC's by TEMPO-mediated reaction (NFCT's). The nanocellulose suspension and gels are characterized by FTIR at ATR mode, TGA, XRD, TEM, SEM, X-ray computed microtomography (micro-CT) and DMTA. The addition of CNC's, NFC's, CNCT's or NFCT's in the microstructure of gels increases their dimensional stabilities. The best results are obtained when CNCT's and NFCT's are added. The mechanical properties and dimensional stability of *Alg/Ch* semi-IPN's increase after controlled thermal post-treatment. The heating during thermal post-treatment boosts the physicochemical interactions in the microstructures of semi-IPN's. The biological assays show biocompatibility of fibroblast cells on the substrates, and differentiation and proliferation up seven days. The optimized mechanical properties, dimensional stability and biocompatibility of the gels studied in this work are important parameters for potential biomedical applications of these biomaterials.

Highlights

Advanced applications of hydrogels in biomedical fields

Nanomaterials for biomedical applications

Bio-based polymers and their biocompatibility in human body

Green chemistry and unexpensive and exotic materials in emerging countries

Optimization of laboratory trials for industrial scale-up

Introduction

Synergistic effects arise when polymers are blended to prepare interpenetrating or semi-interpenetrating polymer networks also known as IPN's or semi-IPN's, respectively. These polymer networks enable preparation of materials and controlled and advanced properties (Naseri et al., 2016). The chitosan (*Ch*) is a polyelectrolyte obtained by physicochemical modification reaction of chitin and generally used to prepare biocompatible substrates (Li et al., 2005; Zhou, 2011). The alginate (*Alg*) is an anionic polyelectrolyte naturally biosynthesized by brown algaes. The *Ch* and *Alg* are some main polyelectrolytes used to prepare biocompatible materials.

The polyelectrolyte complexes (PEC's) or polyelectrolyte macroion complexes (PMC's) are prepared by the mixture of oppositely charged polymers. They can be used to prepare multifunctional hydrogels and to obtain tunable physicochemical properties (Gabrovska et al., 2008). The microstructure of the hydrogels are kept mainly by electrostatic interactions. However, these kind of interactions are highly dependent of pH and ionic strength of the reaction medium (Berger et al., 2004).

The *Ch* is a well known polymer due to its properties as biodegradability, biocompatibility and antimicrobiological activity (Lohani et al., 2014; Rinaudo, 2008). This polyelectrolyte is used in biomedical fields due to its ability to accelerate wound healing (Czaja et al., 2007). The *Ch*-based hydrogels can be prepared by crosslinking between tripolyphosphate and vinyl alcohol and functional groups of *Ch* chains (Berger et al., 2004). The microstructure of physically crosslinked *Ch*-based hydrogels are kept by electrostatic interactions between the negative charges of the crosslinking agents and positive charges of amine functional groups of *Ch* structure. However, the mechanical properties and dimensional stability of physically crosslinked hydrogels are limited by the charge density of the crosslinking agent and polyelectrolytes, the ionic strength and pH of the medium (Azzam et al., 2016).

The covalently crosslinked hydrogels present strong bonds and three-dimensional networks (Senna et al., 2014; Senna and Botaro, 2017). The microstructure of these hydrogels allows effective diffusion of fluids and a minimum decrease of their mechanical properties and dimensional stability. These hydrogels show applications in biomedical fields, as for example, drug delivery systems and to prepare scaffolds. One drawback to use covalent crosslinking agent to prepare hydrogels is its degree of biocompatibility. Glutaraldehyde and glyoxal are good candidates as covalent crosslinking agents of *Ch* but they present neurotoxic (Betancor et al., 2006) and mutagenic effects (Murata-Kamiya et al., 1997). The genipin is an interesting natural and crosslinking agent to replace dialdehydes to prepare covalently crosslinked hydrogels (Mi et al., 2002). This chemical is an aglycone derived from iridoid glycoside also called geniposide and presents good cytocompatibility. However, the use of genipin in large scale is limited by its high price and limited availability in the nature.

Some studies show effectiveness to improve the properties of *Ch*-based hydrogels through the formation of semi-IPN's or IPN's. These materials can be obtained by mixture of *Ch* and *Alg* at controlled conditions. The semi-IPN gels have taken considerable attention of the scientific community due to their improved properties obtained by synergistic effects (Berger et al., 2004; and Lohani et al., 2014). The *Ch*-based semi-IPN gels have also been described more effective during cell culture assays than gels prepared only from *Ch* (Berger et al., 2004).

Rani et al. (2011) describe the controlled drug release of chitosan/glycine/glutamic acid IPN gels crosslinked by glutaraldehyde. Their results were promising for biomedical applications. It was observed that the degree of swelling and releasing of drugs are limited by the pH, the degree of crosslinking in the IPN structure and weight ratio (wt%) of the polymers. Reddy et al. (2009) synthesized chitosan/ghatti gum IPN's by the emulsion technique and glutaraldehyde as crosslinking agent. The microparticles were

used for controlled release of sodium diclofenac. It was observed drug releasing up to 12 h in the intestine.

Li et al. (2009) show the cytocompatibility and cell viability of chitosan/alginate scaffolds. The cell morphology, proliferation and bioadhesion on the material were studied *in vitro*. The analyzes of proteins extracted during cell growth showed the production of a specific type of collagen. This behavior was not observed on the crosslinked *Ch*-based substrate itself. This study suggests that chitosan/alginate semi-IPN's enable cell proliferation, increase the expression of the HTB-94 chondrocyte phenotype and can be used as an alternative to prepare scaffolds. However, any mechanical measurement was described.

Rani et al. (2011) carried out the synthesis of chitosan/alginate semi-IPN's to be used as scaffolds. Silver nanoparticles were added in the microstructure as antibacterial agent. It can be postulate based on their results the potential use of this kind of material in biomedical areas and the needs of complementary studies as mechanical and thermal properties, and porous microstructures of chitosan/alginate hydrogels.

The first part of our research project was published in a recent paper (Siqueira et al., 2019) in which was studied alginate/nanocelluloses hydrogels. This article can be considered primary studies towards optimization of thermal and mechanical properties, experimental procedures and biological features. The alginate/nanocellulose hydrogels were submitted to cytotoxicity and biocompatibility assays. However, the use of sodium alginate presents some limitations as price, synthesis, availability and mechanical properties. Based on these assumptions additional studies to improve or to impart new properties into these materials are needed.

In this study it was decided to add chitosan (cationic polyelectrolyte) and alginate (anionic polyeletrolyte) to prepare semi-interpenetrating polymer networks (semi-IPN's) and nanocelluloses to optimize the material, to impart new properties and to increase some others not presented when only alginate and nanocelluloses were used to prepare biomaterials. Some advantages of the blend between these polyelectrolytes are related to economical concerns (actually the price of alginate is 1.5 higher than chitosan), mechanical properties and biocompatibility effects (*Ch* is a polyelectrolyte derived from chitin which present impressive properties and interesting biocompatibility).

The material prepared by alginate/chitosan presents classical and rich theoretical and experimental information about physicochemistry domains and the drawbacks related to its preparation. This article putt other readers at close contact with very important theories (physycochemistry of solution, suspension, and polyelectrolytes; colloidal sciences; and surface and interface physicochemical interactions, etc.) to prepare advanced materials, and the experimental limitations related by the structures of these chemicals at molecular level.

CNC's and NFC's were added in the gels at different mixture order, pH, ionic strength and concentration in this work. Un- and modified nanocelluloses (TEMPO oxidized) were used to increase or to impart new

properties. It is expected that the careful empirical studies and characterization techniques evidence the benefits and synergistic effects between the components of the semi-IPN's.

The addition of nanocelluloses in *Alg/Ch* semi-IPN's, mainly oxidized cellulose nanocrystals and nanofibrils (CNCT's and NFCT's, respectively) presented the very promising results. These features are very important for structural applications, transport of biological fluids and nutrients; and cell attachment, growth, differentiation and proliferation. To the best of our knowledge any study was still published describing all these parameters (biocompatibility, addition of un- and modified nanocelluloses, mechanical and thermal properties, dimensional stability, porous structures and physicochemical interactions). These materials also present remarkable ecological and economical concerns and advances towards sustainability and green chemistry.

The *Ch* is a polyelectrolyte slightly soluble in water and potential candidate for application in biomedical engineering. Its structure is formed by β-(1-4)-2-amino-2-deoxy-D-glucose units. The polymer chains of *Ch* are similar to cellulose and in acidified medium *Ch* is a polycation due to protonation of amine groups. The *Alg* is an anionic polyelectrolyte and its linear chain is soluble in aqueous media. The *Alg* is well known due to their healing and anti-tumoral properties. It consists of β-D-manuronic acid (M) and α-L-guluronic acid (G) units linked by glycosidic bonds. *Alg* is considered a polyanion at neutral or alkaline medium due to carboxyl groups in its structure.

The physicochemical interactions between *Alg* and *Ch* mainly through electrostatic interactions is a challenge. This blend can be an interesting candidate to prepare stable hydrogels and to impart improved structural homogeneity, dimensional stability and mechanical and biological properties when compared to other prepared from *Alg* or *Ch* themselves or by polymers derived from sources as petroleum (Li et al., 2005).

Materials And Methods

Materials

The bleached *Eucalyptus* pulp used in this work was supplied by Suzano Papel e Celulose (Brazil). Sodium hypochlorite (NaClO), 2,2,6,6-tetramethylpiperidin-1-oxyl solution (TEMPO radical at 98%), sodium bromide (NaBr), hydrochloric acid (HCl at 37%), sulfuric acid (H_2SO_4 at 98%) and sodium hydroxide (NaOH) were used. All these chemicals were supplied by Sigma Aldrich.

The hydrogels were prepared with *Alg* of high molecular weight supplied by Sigma-Aldrich (M_w = 1 x 10^6 $g.mol^{-1}$, M/G ratio = 1.56 and viscosity of 250 cP at 25°C and 2 wt%). The *Ch* was supplied by Phytomare (M_w < 100 kDa and average degree of deacetylation of 90%). Glacial acetic acid ($C_2H_4O_2$ at 99.8%) and calcium chloride ($CaCl_2.2H_2O$) were purchased of Vetec Química Fina Ltda (Brazil).

The phosphate buffer solution (PBS) was prepared by mixture of sodium chloride (NaCl), potassium chloride (KCl) and potassium phosphate (K_3PO_4). All these chemicals were supplied by Synth. The

sodium phosphate monohydrate ($Na_3PO_4.H_2O$) supplied by Vetec Química Fina Ltda and orthophosphoric acid (H_3PO_4 at 85%) supplied by Neon. All these chemicals were supplied at pure degree and used as received.

Methods

Extraction, oxidation reaction and characterization of nanocelluloses

The cellulose nanofibrils (NFC's) and nanocrystals (CNC's) were extracted and isolated, respectively, from bleached kraft cellulose pulp.

The NFC's were obtained from mechanical shearing. The bleached cellulose fibers were suspended in water at 2 wt% and grounded in a Supermass Colloider mill (MKZA10-20J CE Masuko Sangyo, Japan).

The CNC's were also obtained from bleached kraft pulp in the Laboratory of Physicochemistry of UFMG (Brazil). The hydrolysis reaction was carried out in sulfuric acid solution at 65% (v/v), 50^oC and constant mechanical stirring for 50 min. Three dilutions were performed with milli-Q water to stop the reaction. The suspension was submitted to centrifugation steps to remove the excess of acid. The supernatant was eliminated and the precipitate solubilized, and added in dialysis membranes. Changes of water of dialysis bath were carried out up to neutral pH. The suspension of CNC's was submitted to ultrasound treatment for 2 min (Unique Sonicator, 40 kHz) and filtered through membranes of acetate cellulose (Sartorius).

The NFC's and CNC's were oxidized by TEMPO catalyzed reaction. The oxidation of hydroxyl groups in nanocelluloses was performed based on the method described by Saito and Isogai (2004).

Cellulose pulp at 1.5 wt% was used to prepare TEMPO-oxidized cellulose nanofibers (NFCT's). It was added 0.016 g of TEMPO radical in the aqueous reaction medium, 0.100 g of NaBr and 5.35 mL of NaClO at 14 wt%. The pH of the medium was kept at 10 by addition of sodium hydroxide solution. The NFCT's were washed by distilled water and centrifugation steps up to neutral pH. At the end suspensions at 2 wt% of NFCT's were obtained.

Suspension of TEMPO-oxidized cellulose nanocrystals (CNCT's) was prepared based on the experimental procedures described by Saito et al. (2007). The 0.100 mmol TEMPO radical and 1.00 mmol NaBr were solubilized in water per gram of cellulose. The suspension of CNC's at 2 wt% were added into a three bottom neck flask. The pH of the suspension was kept at 10 by the addition of sodium hydroxide solution. The oxidation reaction was started by addition of sodium hypochlorite (NaClO). The CNCT's were washed by centrifugation steps and putted in dialysis membranes (6-8 kDa) up to neutral pH.

Conductometric titrations were performed as described by Saito and Isogai (2004) to determine the degree of oxidation (DO) of the nanocelluloses. Approximately 50.0 mg of TEMPO oxydized nanocelluloses were suspended in 0.0500 $mol.L^{-1}$ hydrochloric acid solution and the pH adjusted up to

2.7 to protonate acid groups present on the nanocelluloses. The titration was carried out by dropwise of 0.0100 mol.L^{-1} sodium hydroxide solution.

Alg/ Ch semi-IPN's

To prepare *Alg/Ch* semi-IPN's a three-dimensional network is desirable between carboxylic groups in *Alg* and amine groups in *Ch* structure. Some physicochemical interactions, as for example between divalent metal cations (M^{2+}), as calcium ions, and negatively charged groups as carboxylate contribute to the formation of the microstructure. *Alg/Ch*/nanocellulose gels were prepared in aqueous media. Both polyelectrolytes present ionic functional groups in their chains at specific experimental conditions. This is possible at the pH close to the pKa values of the functional groups (Azzam et al., 2016; Li et al., 2009; Siqueira et al., 2019; Saito et al., 2007; Saito and Isogai, 2004; Senel et al., 2000). The *Alg* shows pKa value in the range of 3.38 and 3.65 for sequences of M and G, respectively, and *Ch* pKa value close to 6.3. In this work the optimized pH to prepare PEC's and semi-IPN's is in the range between 3.4 and 6.3. It was decided to use an optimized pH of 5.3 after trials.

The *Alg*- and *Ch*-based gels were also crosslinked by calcium ions (Ca^{2+}) to enable comparative data (blank samples). The *Ch* solution was prepared at pH 5.3 and 2.0 wt% and *Alg* solution at pH 3.8 and 2.0 wt%. The *Alg* and *Ch* solutions were slowly added under mild mechanical stirring (340 rpm) at 60^{o}C for 60 min. The PEC's were cooled in liquid nitrogen and freeze dried for 48 h. The gels were added in a bath of 2.0 wt% of calcium chloride solution for 15 min. At this time the interactions between negatively charged groups (carboxylate groups) and Ca^{2+} can takes place and the microstructure of *Alg/Ch* semi-IPN's be formed. It is worth pointed out that trials to determine an optimized contact time of *Alg/Ch* semi-IPN's in calcium chloride solution bath were previously performed (between 5 min and 24 h). The *Alg/Ch* semi-IPN's crosslinked by calcium ions were washed in distilled water to remove excess, cooled in liquid nitrogen and freeze dried for 48 h.

Nanocellulose suspensions at 1.14 wt% were first dispersed in sodium *Alg* solution (2.0 wt%) for synthesis of *Alg/Ch/nanocellulose* semi-IPN's. The weight ratio between nanocelluloses, *Alg* and *Ch* in these studies are shown in Table 1. These mixtures were also kept under heating and stirring for 60 min, cooled and freeze dried for 48 h. The gels were added in 2.0 wt% calcium chloride bath for 15 min. The crosslinked materials were washed by distilled water to remove excess of calcium ions and freeze dried for 48 h.

Tab. 1: Weight ratio of nanocelluloses (wt%) for synthesis of *Alg/Ch* semi-IPN's.

Sample	*Ch (g)*	*Alg (g)*	Nanocelluloses *(g)*	*Alg/Ch*/nanocelluloses
Alg/Ch	0.20	0.20	0.00	0.00
Alg/Ch/CNC10	0.20	0.20	0.04	0.10
Alg/Ch/CNC36	0.20	0.20	0.22	0.55
Alg/Ch/CNC50	0.20	0.20	0.40	1.00
Alg/Ch/CNCT10	0.20	0.20	0.04	0.10
Alg/Ch/CNCT36	0.20	0.20	0.22	0.55
Alg/Ch/CNCT50	0.20	0.20	0.40	1.00
Alg/Ch/NFC10	0.20	0.20	0.04	0.10
Alg/Ch/NFC36	0.20	0.20	0.22	0.55
Alg/Ch/NFC50	0.20	0.20	0.40	1.00
Alg/Ch/NFCT10	0.20	0.20	0.04	0.10
Alg/Ch/NFCT36	0.20	0.20	0.22	0.55
Alg/Ch/NFCT50	0.20	0.20	0.40	1.00

*Alg/Ch/Nanocelluloses10: 10% of nanocelluloses and 90% of alginate/chitosan; Alg/Ch/nanoceluloses36: 36% of nanocelluloses and 64% of alginate/chitosan; and Alg/Ch/Nanoceluloses50: 50% of nanocelluloses and 50% of alginate/chitosan.

Characterization of nanocelluloses, alginate (*Alg*), chitosan (*Ch*) and *Alg/Ch* semi-IPN gels

Fourier Transformed Infrared Spectroscopy at Attenuated Total Reflection mode (FTIR-ATR)

The infrared spectra of nanocelluloses, polyelectrolyes and semi-IPN's were recorded in a spectrometer (Perkin-Elmer Spectrum) at room temperature. The parameters were wavelength range between 4000 and 500 cm^{-1}, resolution of 2 cm^{-1} and 20 accumulation scans.

Thermogravimetric Analysis (TGA)

Thermogravimetric analyzes of nanocelluloses and hydrogels were performed in a TGA– DTG-60 (Shimadzu) and in alumina crucibles. The analyses were performed at heating rate of 10°C.min^{1} and in

the temperature range between 25 and 600°C. A nitrogen flow of 200 mL.min^{-1} was used during the scans.

X-ray diffraction (XRD)

The nanocelluloses and gels were analyzed by X-ray diffraction (diffractometer Shimadzu model XRD-6000). The parameters used were Cu Kα radiation (λ = 0.155428nm), voltage of 30 kV and current of 30 mA. The spectra were collected in the scanning mode of 2º.min^{-1} at Bragg angle (2θ) range between 5 and 50º.

Dynamic Mechanical Thermal Analyses (DMTA)

The mechanical properties of the gels were studied by DMTA (Netzch model 242). The analyses were carried out in the temperature range between 20 and 80ºC, heating rate of 3ºC.min^{-1}, 1 Hz frequency and initial load of 5 N. Two trials were carried out to study the thermomechanical properties of the samples: i) the samples were submitted to heating-cooling/heating-cooling cycles in the furnace of the apparatus (25-80ºC/25-80ºC); and ii) the samples were thermally post-treated in an oven at 80ºC for 4 h and after analyzed by DMTA. The storage and loss moduli (E' and E", respectively) were obtained from the viscoelastic behavior of the samples.

Scanning Electron Microscopy (SEM)

The morphological characterization of gels was performed in a double-beam scanning electron microscope (FEI Quanta FEG 3D). The samples were cooled in liquid nitrogen to avoid deformation of the gels during fracture. These samples were fixed on supports and coated by carbon films of approximately 15 nm of thickness. The images were recorded at secondary electron mode and acceleration voltage of 20 kV. The micrographs obtained by SEM were also used to determine the average size of pores in the gels with the Image J software. Fifteen measurements were taken in each sample.

X-ray computed microtomography (micro-CT)

Analyses of the three-dimensional morphology of the samples were carried out after cryo-facture in liquid nitrogen in a microtomograph (SkyScan 1174 Bruker, Germany). The parameters used were 50 keV and 40 W of tungsten X-ray source. A CCD camera of 1.3 megapixel resolution was attached to the lens scintillator with a 1:6 zoom range. Projections were recorded between 0 and 360° at an angular increment of 0.50°. It were studied samples of *Alg*/Ch and CNCT's or NFCT's (at 50 wt%). A cross-section of approximately 12 mm edge length was selected and analyses recorded at 40 kV and 800 μA. The pixel size of approximately 10 μm was reached. Image reconstruction was performed using the Feldkamp algorithm. The visualization and quantitative analysis of the volumes were carried out with Thermo Scientific Avizo software (Thermo Fisher Scientific, Oregon - USA).

Biological Assays

The biocompatibility and cytotoxicity of L929 fibroblast cells on *Alg/Ch* semi-IPN's will be published as soon as possible. This article presents indirect evidences of the potential use of these materials through analyses of bioadhesion and cell differentiation obtained from SEM images. The fibroblast cells were cultured on the surfaces of semi-IPN's. Samples of (5x5x1) mm^3 were submitted to sterilization by ultraviolet radiation for 30 min. The gels were immersed in fetal bovine serum (FBS) for 1 h and added into cell suspension ($5x10^6$ $cells.mL^{-1}$). The cell cultures were incubated at 37ºC for 7 days in CO_2 atmosphere. The gels were washed with phosphate buffer solution (PBS). The samples were immersed in ethanol and dried in desiccator with vacuum, coated by thin films of gold and observed in a SEM (Quanta FIB EGF 3D with FEI).

Results And Discussion

It is described in the literature that negatively charged carboxylate groups of *Alg* and positively charged amine groups of *Ch* interact in optimized physicochemical conditions. These polyelectrolytes give rise formation of polyelectrolyte macroion complexes (PMC's) also known as polyelectrolyte complexes (PEC's) (Berger et al., 2004; Isogai et al., 2011). It was used in this work *Alg* and *Ch* as polyelectrolytes and calcium chloride ($CaCl_2$) as crosslinking agent to prepare biocompatible materials due to economic and ecological concerns and towards a green chemistry.

Figure 1 depicts ionic and/or secondary interactions in the microstructure of *Alg/Ch* and *Alg/Ch/*nanocellulose semi-IPN's. It is expected at least some types of interactions as: ionic or electrostatic interactions of carboxylate groups in *Alg* structure and calcium ions; interactions of carboxylate groups in TEMPO-oxidized nanocelluloses, carboxylate groups of *Alg* chains and calcium ions; secondary interactions (hydrogen bonds, van der Waals, induced and permanent dipole) of functional groups in the structure of *Alg*/ *Ch*/nanocelluloses; ionic/electrostatic interactions of *Alg and Ch*; and ionic/electrostatic interactions of carboxylate groups of CNCT's and NFCT's and amine groups of *Ch*.

As stated and well explained and justified by French (2017) the repeating unit of cellulose is often considered to be cellobiose instead of glucose. This review presents some arguments regarding the repeating unit in cellulose molecules and crystals based on biosynthesis, shape, crystallographic symmetry, and linkage position. The statement that cellobiose could be the repeating unit of cellulose instead of glucose needs take some care when regarding the chemical bonds in the structure, reactivity and properties (Nishiyama et al. 2002; Kouwijzer et al. 1995). There is almost universal agreement that cellulose is a polymer of β-(1-4)-linked D-glucopyranosyl units and glucose is repeatedly added during biosynthesis of cellulose chains. One common argument used by some authors to consider cellobiose as the repeating unit of celullose is due to the fact that cellobiose is obtained by hydrolysis of cellulose. However, cellobiose is one of the products of acid hydrolysis and prolonged hydrolysis results at glucose. One report (JCBN, 1982) states that "polysaccharides composed of only one kind of monosaccharide are described as homopolysaccharides" and another report (JCBN, 1983) adds a statement that "The repeating unit in a homopolysaccharide is a sugar residue". This review support the glucose residues as

the repeating unit of cellulose and also in agreement with International Union of Pure and Apllied Chemistry (IUPAC) and International Union of Biochemistry and Molecular Biology (IUBMB).

It's worth pointed out that Figure 1 is just an attempt to describe the complex structure of *Alg/Ch*/nanocellulose semi-IPN's, and possible physicochemical interactions between their components. Any picture could describe completely the microstructure formed. In this paper it was considered glucose as the repeating unit of cellulose to prepare these pictures even if some between then present more than one glucose unit. The pictures are based on articles that describe the egg-box model as one possibility to explain these interactions. One possibility is the formation of dimers around cation ions added in polyelectrolyte solutions to prepare hydrogels (Li et al., 2007; Donati et al., 2005).

Fig. 1: Physicochemical interactions of *Alg*, *Ch* and nanocelluloses in the microstructure of the gels: (A) ionic crosslinking of *Alg* and calcium ions; (B) ionic crosslinking of *Alg*, TEMPO-oxidized nanocelluloses and calcium ions; (C) secondary interactions of the functional groups of *Alg*, *Ch* and nanocelluloses; (D) ionic interactions of *Alg* and *Ch* groups; and (E) ionic interactions of negatively charged groups of CNCT's and NFCT's and positively charged groups of *Ch* chains.

The materials synthesized can be considered physical gels due to reversible feature of the interactions in their microstructures (non-covalent bonds). Figure 2 presents images of the morphology and dimensional stability of the *Alg/Ch/nanocellulose* semi-IPN's after optimization of physicochemical parameters as mixing order, concentration, pH, ionic strength and temperature. The Support Information (SI_1) shows the photographs of *Alg/Ch* semi-IPN's without addition of nanocelluloses.

Fig. 2: Images of gels after freeze drying: (A) and (B) *Alg/Ch*/NFCT (at 50 wt%); and (C) and (D) *Alg/Ch*/CNCT (at 50 wt%).

The freeze-dried and thermally post-treated gels present good dimensional stability. However, their surface areas show some insights. The surface of gel at contact with the mold and air during preparation present smooth and rough surfaces, respectively. The microstructure shows slow shrinkage after thermal post-treatment at 80^{o}C for 4 h, but the materials still kept their dimensional stabilities. It is worth pointed out that porous structures and rough surface areas are very interesting for nutrient flux and cell attachment, respectively. The shrinkage of some samples is probably due to water elimination, reconformation of polyelectrolytes (extended-coil interconversion), and increase of ionic crosslinking density or secondary interactions in the microstructure of the gels. All these phenomena can contribute to decrease the distance between components in the microstructure and to increase physicochemical interactions between them (ionic, electrostatic, van der Waals, permanent and induced dipole). The microstructure is kept intact when compared with the gels without addition of nanocelluloses. After some optimization studies it were added 36 and 50 wt% of nanocelluloses to prepare dimentionatly stable *Alg/Ch/nanocellulose* semi-IPN's.

Figure 3 presents FTIR at ATR mode analyses of *Alg* and *Ch* polyelectrolytes (Figure 3.A) and ionic crosslinked *Alg/Ch/*nanocellulose gels (Figure 3.B). The Support Information (SI_2) shows FTIR spectra for

un- and oxidized nanocelluloses. The high degree of desacetylacetion of *Ch* used in this work (*ca.* 93%) to prepare the gels enables electrostatic interactions between *Alg* and *Ch*, and gives rise the formation of semi-IPN's whose present good dimensional stability in water and phosphate buffer solution (PBS). The blend *Alg/Ch/*oxidized nanocellulose semi-IPN's show better results. The addition of nanocelluloses at 36 and 50 wt% were beneficial to keep the dimensional stability. The ionic crosslinking due to calcium ions was also important for interactions in the *Alg* and *Alg/*nanocellulose phases (calcium ions/carboxylate groups). The interactions between the crosslinked *Alg* or Alg*/*nanocelullose phases and *Ch* phase allow formation of a complex and pore network in the gel microstructures. As can be observed in the FTIR spectra all the main absorption bands of *Alg*, *Ch* and nanocelluloses are also observed in the spectra of each constituent itself even if some bands show overlapping or small displacement of wavelength absorption. These spectra show evidences of ionic or secondary interactions and formation of physical gels. Any new absorption band was observed when the components and the blends are compared which is an evidence that covalent bonds were not formed (chemical gels).

Fig. 3. (A) FTIR spectra at ATR mode of *Alg* and *Ch* polyelectrolytes and (B) crosslinked *Alg/Ch/*nanocellulose semi-IPN's.

The main absorption bands of crosslinked *Alg* are a broad absorption band in the wavelength of 3600 and 3200 cm^{-1} attributed to stretching vibrations of O-H groups; an absorption band at 2900 cm^{-1} attributed to the stretching vibration of the C-H bonds of methyl groups; and two intense absorption bands of carboxyl groups ($-COO^-$) at 1600 and 1411 cm^{-1} attributed to asymmetric and symmetric vibrations, respectively (Siqueira et al., 2019).

The main absorption bands of *Ch* are broad absorption bands in 3600 and 3300 cm^{-1} attributed to axial stretching vibration of -OH and –NH groups; the absorption bands at 2940 and 2880 cm^{-1} attributed to symmetric and asymmetric axial vibration of –CH groups, respectively; an intense absorption band at 1660 cm^{-1} attributed to stretching vibration of C=O (amide I) that overlaps the absorption band at 1586 cm^{-1} attributed to stretching vibration of –NH groups; an absorption band at 1419 cm^{-1} attributed to axial stretching vibration of C-N that overlaps the band at 1377 cm^{-1} attributed to angular stretching vibration of –NH groups. In the wavelength region of 1200 and 800 cm^{-1} the absorption bands of *Alg* and *Ch* are attributed to polysaccharide moieties.

The nanocellullose spectra (SI_2) show some main absorption bands at 3300 cm^{-1} attributed to stretching vibrations of –OH groups; at 2900 cm^{-1} attributed to stretching vibrations of –CH groups; at 1610 and 1411 cm^{-1} attributed to symmetric and asymmetric stretching vibrations of carboxylate groups, respectively; and at 1430 cm^{-1} attributed to stretching of methyl groups. The absorption bands in the range 1200 to 920 cm^{-1} are attributed to stretching vibrations of the polysaccharide structures as also observed in *Alg* and *Ch* spectra (Azzam et al., 2016).

There are some evidences that the interactions between *Alg*, *Ch* and nanocelluloses are secondary interactions based on FTIR analyses. In this work the *Alg/Ch/*nanocellulose gels show broadening and overlapping of the absorption band at 1600 cm^{-1} attributed to stretching vibrations of carboxyl and amine groups. Other evidence is observed at 1400 cm^{-1} also attributed to carboxyl and amine groups. The absorption band in the range 3200 to 3600 cm^{-1} shows a broadening in *Alg/Ch*/nanocellulose gels. This band is attributed to stretching vibrations of –OH and –NH groups, and hydrogen bonds. The displacement and overlapping of characteristic absorption bands of *Alg*, *Ch* and nanocelluloses when compared to the absorption bands of the gels are evidences of secondary interactions between functional groups (mainly carboxylate and amine). Any new absorption band was observed in the gels spectra as postulated before. The high charge density of these polyelectrolytes give rise mainly to formation of physicochemical interactions between them as also observed by Lawrie et al. (2007).

Figure 4.A presents X-ray diffractogram patterns of *Alg* and *Ch,* and Figure 4.B crosslinked *Alg/Ch* and *Alg/Ch*/nanocellulose gels at 50 wt% concentration. The diffractograms show characteristic patterns of polymer materials (when compared as for example with the fine and well defined patterns for metallic or ceramic materials), and more specifically polysaccharides structures (French, 2014).

The *Ch* diffractogram shows two main peaks at aproximatelly 2θ = 10.3° and 19.8° attributed to hydrated and anhydrous crystals, respectively (Li, X., et al., 2009; Chen et al., 2008). The *Alg* presents broaden diffraction peaks attributed to guluronic (G) and manuronic (M) blocks. The main peaks at approximately 2θ = 13.4° (110) and 22.9° (002) are attributed to diffraction plans crystalline regions of *Alg* (Li et al., 2007).

The nanocelluloses present main peaks at approximately 34.5º (004), 22.6º (200), 16.5º(110) and 14.5º (1-10) (Zeng et al.,2021; Siqueira et al., 2019; French, 2017 and 2014; Sun et al., 2016; Brito et al., 2012; Lahiji et al., 2010; Pääkö et al., 2007).

XRD patterns can show small displacements of 2θ values, intensity and/or crystalline/non-crystalline ratio when articles are compared due to experimental procedures, physicochemical parameters for synthesis of polymers or cellulose source for extraction of CNC's and preparation of CNF's.

Some tools as the software and model used during data interpretation and the experimental parameters for sample preparation and parameters for XRD analyses can also affect the results. As one example and stated by French (2014) the patterns calculated by Mercury® program are isotropic but there is no way to input crystallite shape information that can affect the relative peak heights and widths.

In this work X-ray analyses are used for comparison purposes, and to take some additional qualitative information about the microstructural organization of the complex blends between un- and crosslinked *Alg*/ *Ch*/nanocelluloses to prepare hydrogels and their biocompatibility. Attempts to take quantitative information on XRD analyses will be issues of future works as well as cell viability and other correlations between microstructure and biological features.

Figure 4. X-ray diffractograms: (A) alginate and chitosan; and (B) crosslinked *Alg/Ch*/nanocellulose semi-IPN gels.

As observed crosslinked *Alg/Ch* gels and mainly *Alg* diffractogram pattern without addition of nanocelluloses have broaden diffraction peaks suggesting defective crystallization and probably low crystallinity.

Smitha et al. (2005) stated based on their studies that the mixture of *Alg* and *Ch* decreases the crystallinity when compared to the crystallinity of this polymers. The crosslinked *Alg/Ch* gels show lower cristallinity than pure *Ch* and *Alg* probably due to fast physicochemical interactions with calcium ions and the gelation process.

Li et al. (2009) observed that typical peaks of *Ch* disappeared after mixture with *Alg* and the PEC's showed an amorphous morphology similar to *Alg*. It was stated that the introduction of *Alg* into *Ch* disrupted the crystalline structure of *Ch*.

Li et al. (2007) also observed by XRD analyses formation of junction zones with different crystallinity in Ca-alginate gels. This was confirmed by the measurements of Ca-alginate gel beads prepared at different pH and slow crosslinking rate, which leads to a higher crystallinity and more perfect ordering. Reversible aggregation of junction zones and their impacts on XRD patterns were also observed during dehydration and rehydration (or swelling).

Nagahama et al. (2009) observed based on XRD results that there was good compatibility and interaction between gelatin and chitosan molecules in the membranes synthesized. The peak intensity ratio of chitosan membrane was reduced when gelatin was added. A little decrease in the crystallinity of chitosan/gelatin membranes was attributed to formation of hydrogen bonds.

After addition of CNC's, CNCT's, CNF's and CNFT's in Alg/Ch gels at 50 wt% is observed a more perfect ordering, characteristic peaks of these nanostructures and diffractogram patterns more representative of high crystallinity. These results corroborate with a more uniform and organized microstructure and probably formation of hydrogen bonds and ionic interactions between un- and oxidized nanostructures and *Alg/Ch*-based gels.

The thermal stability of *Alg*, *Ch* and *Alg/Ch*/nanocellulose semi-IPN's were analyzed from TGA-DTG curves. The Figures in SI_3 present the curves of TGA obtained in nitrogen atmosphere and their first derivative (DTG). It was observed three main events of weight loss. The first one takes place between 20 and 175ºC and approximately 15% of weight loss attributed to water elimination and small fragments of glycoside structures. The second one in the range of 175 to 385ºC and *ca*. 40% weight loss can be considered the main event. It is attributed to degradation reactions of glycoside structure of *Alg* and *Ch* polyelectrolytes and nanocelluloses. The third one at approximately 385ºC is attributed to degradation of the crystalline regions of these components whose are more thermally stable. It is worth pointed out that in synthetic air or oxidant atmosphere the degradation of glycoside-based structures is generally

displaced towards lower temperatures than nitrogen atmosphere. The residues (ash content) at approximately 600ºC are probably due to calcium inorganic salts as also described by Han et al. (2010).

The thermal degradation of glycoside-based structures was also studied by other authors. The presence of hemicelluloses in the structure of NFC's can displace the temperature of thermal degradations towards lowest values mainly in oxidant atmosphere (Yang et al., 2007). Isogai et al. (2011) describe the formation of sodium carboxylates in the structure of TEMPO oxidized nanocelluloses. These functional groups decrease the thermal stability of the nanocelluloses and displace the degradation temperature towards lowest values. In our work an increase of thermal stability and approximately 30 up to 40% of ash content at 600ºC were observed for Alg/Ch semi-IPN's prepared by addition of TEMPO-oxidized nanocelluloses (CNCT's or NFCT's). This can be partially explained by the ionic crosslinking of the carboxylate groups/calcium ions. These ionic or electrostatic interactions can increase the thermal stability of gels and displace the degradation temperatures of the microstructure towards highest values. The two concentrations of nanocelluloses used in this work (36 and 50 wt%) show similar results when studied by FTIR-ATR, DRX and TGA-DTG. However, the better dimensional stability and mechanical properties were observed when 50 wt% of nanocelluloses were added to prepare gels. Based on these results were carried out on *Alg/Ch*/oxidized nanocellulose gels at 50 wt% analyses of DMTA, SEM and X-ray micro CT images and cell growth assays.

Table 2 shows storage moduli obtained by dynamic mechanical thermal analyses (DMTA) of the gels. The samples were thermally post-treated in the furnace of the apparatus during a consecutive heating-cooling/heating-cooling cycle between 25 up to 80ºC. The results were compared at 35, 37 and 42ºC whose are temperatures for some biomedical applications.

Tab. 2: Storage modulus (E') obtained from DMTA curves during heating-cooling/heating-cooling cycles (25-80)ºC/(25-80)ºC (E'_1: storage modulus during first heating/cooling cycle (25-80)ºC; and E'_2: storage modulus during second heating/cooling cycle).

Semi-IPN's	35ºC		37ºC		42ºC	
(50 wt% nanocellulose)	E'_1 (MPa)	E'_2 (MPa)	E'_1 (MPa)	E'_2 (MPa)	E'_1 (MPa)	E'_2 (MPa)
Alg/Ch	0.08	2.50	0.15	3.00	0.30	3.50
Alg/Ch/CNC	0.10	5.88	0.40	6.37	0.80	8.50
Alg/Ch/CNCT	0.10	6.50	0.11	8.10	0.11	10.1
Alg/Ch/NFC	0.10	7.05	0.10	7.20	0.10	8.00
Alg/Ch/NFCT	0.09	6.88	0.10	7.52	0.10	9.01

The biomaterials prepared by natural polymers or their derivatives and biopolymers generally present favorable microstructure for cell bioadhesion and proliferation. The poor mechanical properties and dimensional stability are generally drawbacks for their applications. The storage moduli (E') show low

values during first heating/cooling cycle as observed by DMTA analyses. This can be explained by the polyelectrolyte structures and fast ionic crosslinking in the calcium chloride bath. In these conditions polymer conformation and full ionic crosslinking can be limited before an ultimate state. When thermal post-treatment is carried out the polyelectrolyte structures are submitted to relaxations close to glass transitions values and the polymer chains can approach each other and to interact more effectively. Some additional degree of ionic crosslinking of calcium ions and carboxylate groups of *Alg* and CNCT's and NFCT's is expected. These behaviors (polymer relaxation and conformation and additional ionic crosslinking) can explain the remarkable increase of E' after the first heating cycle up to 80ºC and during the second heating-cooling cycle (Siqueira and Botaro, 2013).

The increase of mechanical properties of semi-IPN's was also observed and described by authors when nanocelluloses are added in some polyelectrolytes (De France et al., 2017; Kumar et al. 2017). It can be observed in this work synergistic effects that increase the mechanical properties when oxidized nanocelluloses are added in the microstructure of gels and controlled thermal post-treatments are performed on the samples.

It was decided to use CNCT's and NFCT's during porosity and cell growth studies after analyses of the influences of thermal post-treatment on the mechanical properties of *Alg/Ch*/nanocellulose semi-IPN's. Even if all nanocellulose based-gels presented improved mechanical properties after thermal post-treatment the best results were observed when TEMPO oxidized nanocelluloses based-gels are submitted to thermal post-treatment for 4 h at 80ºC in an oven. Klemm et al. (2011), Lin and Dufresne (2014) and Chinga-Carrasco (2018) also described the great potential of biopolymer and nanocellulose applications to prepare biomaterials for regenerative medicine and would healing treatments.

Figure 5 presents micrographs obtained by SEM analyses of *Alg/Ch*/nanocellulose semi-IPN's. The pore sizes, their distribution and interconnectivity are very important for effective flow of nutrients and biological fluids. Figure 5.a shows the micrograph of *Alg/Ch* semi-IPN's. It can be observed porous structures and thin walls that are characteristic of alginate-based gels. The addition of nanocelluloses (Figures 5.b-e) enable formation of porous structures and pore sizes in the range of 40 up to 150 µm when compared to gels without addition of nanocelluloses that show pore sizes in the range of 20 up to 40 µm. Li et al. (2005) stated based on their studies that porous substrates in the range of 100 up to 300 µm are beneficial for cell growth and potential biomedical applications.

The gels prepared by addition of nanocelluloses (CNC, CNCT, NFC and NFCT) presented bigger pore sizes and rough walls than gels without them. These features can be partially explained by the impressive properties of nanocelluloses (high surface area, reactivity, stiffness and mechanical properties) (Siqueira et al., 2019; Lin and Duffresne, 2014). The synergistic effects of the addition of nanocelluloses, mainly TEMPO-oxidized, calcium crosslinking and thermal post-treatment improve the mechanical properties and increases the surface available for cell attachment.

Fig. 5. Micrographs obtained by SEM of semi-IPN's at 50 wt% nanocellulose concentration: (A) *Alg/Ch* semi-IPN's, (B) *Alg/Ch*/CNC, (C) *Alg/Ch*/CNCT, (D) *Alg/Ch/*NFC, (E) *Alg/Ch*/NFCT (magnification of 500x;

the insets represent a magnification of 1000x).

Figure 6 shows images obtained by X-ray micro CT of *Alg/Ch*/nanocellulose semi-IPN's. This powerful technique enables to take qualitative and quantitative information of volume, size, shape, distribution and interconnectivity of pores (Isaac et al., 2015). The results corroborate with SEM images as a complementary tool to take some additional information about the internal microstructures of the gels. In this work the results of X-ray micro CT will be used for comparative purposes.

The Figure 6.A shows an oriented structure of pores for *Alg/Ch*/CNCT semi-IPN's and cracks probably due to the stiffness of CNCT's (rigid rod-like structures) added in the gels. The Figure 6.B presents *Alg/Ch*/NFCT semi-IPN's. It can be observed higher pore sizes, more uniform distribution and ribbed and roughness surfaces for these gels than CNCT-based gels.

It was used the software Image J to take some quantitative information when compared *Alg/Ch/*nanocellulose IPN's for comparative purposes and based on the work of Isaac et al. (2015). The CNCT's and NFCT's-based gels present 50 and 80% of pores in their microstructures, respectively. Both oxidized nanocelluloses-based gels showed thickness of pore walls of 16 up to 20 μm but NFCT's-based gels presented the highest homogeneity.

Fig. 6: X-ray micro CT images of gels prepared at 50 wt% concentration: (a) *Alg/Ch*/CNCT semi-IPN's, (b) *Alg/Ch*/NFCT semi-IPN's, and (C) thickness of pore walls of Alg/Ch/nanocellulose semi-IPN's.

It is important for biomedical applications a combined effect of mechanical and biological properties to enable, for example, direct contact or replacement of some tissues of human body. It were carried out cytotoxicity and cell growth assays to analyze the properties of the materials synthesized in this work and their potential biomedical applications. At this time will be show some of the results obtained for cell growth.

Figure 7 shows cell growth assays of L929 fibroblast cells. This kind of cells were cultured on substrates and the best results were observed on *Alg/Ch/*nanocellulose gels (CNCT's and NFCT's at 50 wt%) (Figure 7.C-F) when compared to gels prepared without addition of nanocelluloses (Figure 7.A and B). It can be observed cell attachment, proliferation and differentiation of L929 fibroblast cells mainly on *Alg/Ch*/NFCT IPN's (Figure 7.E and F). The cell growth was observed during all the time of the studies performed in this work (up to 30 days).

The L929 fibroblast cells are attached in the gel microstructure as observed in the micrographs. The rough surface of the gels, the polyelectrolyte charges, the nanocellulose and the pore surface are essential parameters for attachment. The morphology of cells is kept approximately spherical or extended which are some evidences of proliferation, differenciation and/or biocompatibility on the substrate (Dan et al., 2016; Domingues et al., 2014).

It was clearly possible to observe cell attachment of L929 fibroblast cells on *Alg/Ch*/NFCT IPN's mainly due to surface area of the NFCT's and functional groups as carboxylate and amino (Figure 7.E and F).

These groups influence the cell adhesion, proliferation and differentiation due to physicochemical interactions of proteins of L929 fibroblast cells (Rashad et al., 2017). It can be also observed surprisingly the formation of thin and long filaments derived from fibroblast cells that improve the attachment (SI_4). These filaments show high degree of adherence and biocompatibility of the cells on these gels.

Figure 7. Micrographs obtained by SEM of semi-IPN's: (A) and (B) *Alg/Ch*, (C) and (D) *Alg/Ch*/CNCT (at 50 wt%), and (E) and (F) *Alg/Ch*/NFCT (at 50 wt%).

Conclusions

The *Alg/Ch*/nanocellulose semi-IPN's present good dimensional stability and rough surface area, and enable cell attachment, growth, proliferation and differentiation for time interval as long as 30 days. The physicochemical parameters (pH, ionic strength, charge density, order of mixture, oxidation reaction and nanocellulose concentration), ionic crosslinking and thermal post-treatment influences directly the microstructure of the gels as observed by SEM and X-ray micro CT images. The roughness of the surface and complex structure of pores of these gels when nanocelluloses are added collaborate to cell attachment and growth.

Declarations

ACKNOWLEDGEMENT

REDEMAT-UFOP, UFSCar, FAPESP (Processo:16/19896-2 Linha de fomento: Auxílio à Pesquisa - Regular), CNPq and "This study was financed in part by the Coordenação de Aperfeiçoamento de Pessoal de Nível Superior - Brasil (CAPES) - Finance Code 001"

Funding: REDEMAT-UFOP. UFSCar, FAPESP, CNPq and CAPES

Conflicts of interest/Competing interests: Not applicable

Availability of data and material: Not applicable

Code availability: Not applicable

Authors' contributions:

Priscila Siqueira[b]: experimental and analyses

Ana de Lima[a]: experimental and analyses

Felipe Medeiros[a]: experimental and thermal and mecanical analyses

Augusta Isaac[c]: scientific discussions and images analyses

Katia Novack[b]: co-supervisor of the project

Vagner Botaro[d]: supervisor of the project

Éder Siqueira[a]: writing, submission, expeirmental and analyses

The first draft of the manuscript was written by Eder Siqueira and all authors commented on previous versions of the manuscript. All authors read and approved the final manuscript.

Ethics approval The authors declare that they have no known competing financial interests or personal relationships that could have appeared to influence the work reported in this paper.

Consent to participate: All the authors declare to consente participation

Consent for publication All the authors declare to consente publication of this work

References

Azzam, F., Siqueira, E., Fort, S., Hassaini, R., Pignon, F., Travelet, C., Putaux J.-L, Jean, B., Tunable Aggregation and Gelation of Thermoresponsive Suspensions of Polymer-Grafted Cellulose Nanocrystals, Biomac. (2016), 17:2112-2119(https://DOI: 10.1021/acs.biomac.6b00344).

Berger, J., Reist, M., Mayer, J.M., Felt, O., Gurny, R., Structure and interactions in chitosan hydrogels formed by complexation or aggregation for biomedical applications, Eur. J. Pharmac. Biopharmac. (2004), 57:35-52(https://doi.org/10.1016/S0939-6411(03)00160-7).

Betancor, L., López-Gallego, F., Hidalgo, A., Alonso-Morales, N., Mateo, G.D-O.C., Férnandes-Lafunte, R., Guisán, J.M., Different mechanisms of protein immobilization on glutaraldehyde activated supports: Effect of support activation and immobilization conditions, Enzy. Microb. Technol. (2006), 39:877-882(https://doi.org/10.1016/j.enzmictec.2006.01.014).

Brito, S.L., Pereira, F.V., Putaux, J.-L., Jean, B., Preparation, morphology and structure of cellulose nanocrystals from bamboo fibers, Cellulose (2012), 19:1527–1536(https://doi.org/10.1007/s10570-012-9768-9).

Chen, Z., Mo, X., He, C., Wang, H., Intermolecular interactions um electrospun collagen-chitosan complex nanofibers, Carbohyd. Polymers (2008), 72:410–418 (https://doi.org/10.1016/j.carbpol.2007.09.018).

Chinga-Carrasco, G., Potential and Limitations of Nanocelluloses as Components in Biocomposite Inks for Three-Dimensional Bioprinting and for Biomedical Devices, Biomac. (2018), 19:701-711(https://doi.org/10.1021/acs.biomac.8b00053).

Czaja, W.K., Young, D. J., Kawecki, M., Brown, R.M., The Future Prospects of Microbial Cellulose in Biomedical Applications, Biomac. 8 (2007), 1-12(https://doi.org/10.1021/bm060620d).

Dan, Y., Liu, O., Liu, Y., Zhang, Y.-Y., Li, S., Feng, X.-B., Shao, Z.-W., Yang, C., Yang, S.-H., Hong, J.-B., Development of Novel Biocomposite Scaffold of Chitosan-Gelatin/Nanohydroxyapatite for Potential Bone Tissue Engineering Applications, Nano. Res. Let. (2016) 11 (https://doi.org/10.1186/s11671-016-1669-1).

De France, K.J., Hoare, T., Cranston, E.D., Review of Hydrogels and Aerogels Containing Nanocellulose, Chem. Mater. (2017), 29:4609-4631(https://doi.org/10.1021/acs.chemmater.7b00531).

Domingues, R.M.A., Gomes, M.E., Reis, R.L., The Potential of Cellulose Nanocrystals in Tissue Engineering Strategies, Biomac. (2014), 15:2327-2346(https://doi.org/10.1021/bm500524s).

Donati, I., Holtan, S., Mørch, Y.A., Borgogna, M., Dentini, M., Skjåk-Bræk, G., New Hypothesis on the Role of Alternating Sequences in Calcium-Alginate Gels, Biomacromolecules (2005), 6:1031-1040 (https://doi.org/10.1021/bm049306e).

French, A.D., Glucose, not cellobiose, is the repeating unit of cellulose and why that is importante, Cellulose (2017), 24:4605-4609(https://doi.org/10.1007/s10570-017-1450-3).

French, A.D., Idealized powder diffraction patterns for cellulose polymorphs, Cellulose (2014), 21:885-896(https://doi.org/10.1007/s10570-013-0030-4).

Gabrovska, K., Marinov, I., Godjevargova, T., Portaccio, M., Lepore, M., Grano V., Diano, N., Mita, D. G., The influence of the support nature on the kinetics parameters, inhibition constants and reactivation of immobilized acetylcholinesterase, Int. J. Biol. Macromol. (2008), 43: 339-345(https://doi.org/10.1016/j.ijbiomac.2008.07.006).

Han, J., Zhou, Z., Yin, R., Yang, D., Nie, J., Alginate–chitosan/hydroxyapatite polyelectrolyte complex porous scaffolds: Preparation and characterization, Int. J. Biol. Macromol. (2010), 46:199-205(https://doi.org/10.1016/j.ijbiomac.2009.11.004).

Isaac, A., Barboza, V., Sket, F.I., D'Almeida, J.R.M., Montoro, L.A., Hilger, A., Manke, I., Towards a deeper understanding of structural biomass recalcitrance using phase-contrast tomography, Biotechnol. Biofuels (2015), 10:8-40(https://doi.org/10.1186/s13068-015-0229-8).

Isogai, A., Saito, T., Fukuzumi, H., TEMPO-oxidized cellulose nanofibers, Nanoscale (2011), 3:71-85(https://doi.org/10.1039/C0NR00583E).

JCBN (1983) Symbols for specifying the conformation of polysaccharide chains. Recommendations 1981, Eur J Biochem, 131, 5–7; Pure Appl Chem, 55, 1269–1272.

JCBN (1982) Polysaccharide nomenclature recommendations 1980* Pure Appl Chem, 54, 1523–1526; J Biol Chem, 257, 3352–3354.

Klemm, D., Kramer, F., Moritz, S., Lindström, T., Ankerfors, M., Gray, D., Dorris, A., Nanocelluloses: A New Family of Nature-Based Materials, Ang. Chem. Int. Ed. (2011), 50:5438-5466(https://doi.org/10.1002/anie.201001273).

Kouwijzer, M.L.C.E., van Euck, B.P., Kooijman, H., Kroon, J., An extension of the GROMOS force field for carbohydrates, resulting in improvement of the crystal structure determination of α-D-galactose, Acta Crystalloogr Sect B (1995), 51:209–220(https://doi.org/10.1107/S0108768194011262).

Kumar, A., Rao, K.M., Han, S.S., Synthesis of mechanically stiff and bioactive hybrid hydrogels for bone tissue engineering applications, Chem. Eng. J. (2017), 317:119-131(https://doi.org/10.1016/j.cej.2017.02.065).

Lahiji, R.R., Xu, X., Reifenberger, R., Raman, A., Rudie, A., Moon, R.J., Atomic Force Microscopy Characterization of Cellulose Nanocrystals, Langmuir (2010), 26:4480-4488(https://doi.org/10.1021/la903111j).

Lawrie, G., Keen, I., Drew, B., Chandler-Temple, A., Rintoul, L., Fredericks, P., Grondahl, L., Interactions between Alginate and Chitosan Biopolymers Characterized Using FTIR and XPS, Biomac. (2007), 8:2533-2541(https:// doi: 10.1021/bm070014y).

Li, X., Xie, H., Lin, J., Xie, W., Ma, X., Characterization and biodegradation of chitosan–alginate polyelectrolyte complexes, Pol. Degr. Stab. (2009), 94:1-6(https://doi.org/10.1016/j.polymdegradstab.2008.10.017).

Li, L., Fang, Y., Vreeker, R., Appelqvist, I., Reexamining the Egg-Box Model in Calcium-Alginate Gels with X-ray Diffraction Biomacromolecules (2007), 8:464-468(https://doi.org/10.1021/bm060550a).

Li, Z., Ramay, H.R., Hauch, K.D., Xiao, D., Zhang, M., Chitosan–alginate hybrid scaffolds for bone tissue engineering, Biomater. (2005), 26:3919-3928(https://doi.org/10.1016/j.biomaterials.2004.09.062).

Lin, N. and Dufresne, A., Nanocellulose in biomedicine: Current status and future prospect, Eur. Pol. J. (2014), 59:302-325(https://doi.org/10.1016/j.eurpolymj.2014.07.025).

Lohani, A., Singh, G., Bhattacharya, S.S., Verma, A., Interpenetrating Polymer Networks as Innovative Drug Delivery Systems, J. Drug Deliv. (2014), 1-11(https://doi.org/10.1155/2014/583612).

Mi, F.-L., Sung, H.-W., Shyu, S.-S., Drug release from chitosan–alginate complex beads reinforced by a naturally occurring cross-linking agent, Carbohydr Pol. (2002), 48:61-72(https://doi.org/10.1016/S0144-8617(01)00212-0).

Murata-Kamiya, N., Kamiya, H., Kaji, H., Kasai, H., Mutational specificity of glyoxal, a product of DNA oxidation, in the *lacI* gene of wild-type *Escherichia coli* W3110, Mut. Res. Fundam. Mol. Mech. Mutag. (1997), 377:255-262(https://doi.org/10.1016/S0027-5107(97)00083-3).

Nagahama, H., Maeda, H., Kashiki, T., Jayakumar, R., Furuike, T., Tamura, H., Preparation and characterization of novel chitosan/gelatin membranes using chitosan hydrogel, Carbohydrate Polymers (2009), 76:255-260(https://doi.org/10.1016/j.carbpol.2008.10.015).

Naseri, N., Deepa, B., Mathew, A.P., Oksman, K., Girandon, L., Nanocellulose-Based Interpenetrating Polymer Network (IPN) Hydrogels for Cartilage Applications, Biomac. (2016), 17:3714-3723(https://doi.org/10.1021/acs.biomac.6b01243).

Nishiyama, Y., Langan, P., Chanzy, H., Crystal structure and hydrogen-bonding system in cellulose Ibeta from synchrotron X-ray and neutron fiber diffraction, J Am Chem Soc (2002), 124:9074–9082(https://doi.org/10.1021/ja0257319).

Pääkkö, M., Ankerfors, M., Kosonen, H., Nykänen, A., Ahola, S., Österberger, M., Ruokolainen, J., Laine, J., Larsson, P.T., Ikkala, O., Lindström, T., Enzymatic Hydrolysis Combined with Mechanical Shearing and High-Pressure Homogenization for Nanoscale Cellulose Fibrils and Strong Gels, Biomac. (2007), 8:1934-1941(https://doi.org/10.1021/bm061215p).

Rani, M., Agarwal, A., Negi, Y.S., Characterization and Biodegradation Studies for Interpenetrating Polymeric Network (IPN) of Chitosan-Amino Acid Beads, J. Biomater. Nanobiotech. (2011), 2:71–84(https://doi:10.4236/jbnb.2011.21010).

Rashad, A., Mustafa, K., Heggset, E.B., Syverud, K., Cytocompatibility of Wood-Derived Cellulose Nanofibril Hydrogels with Different Surface Chemistry, Biomac. (2017), 18:1238–1248(https://doi.org/10.1021/acs.biomac.6b01911).

Reddy, K.O., Guduri, B.R., Varada Rajulu, A. Structural characterization and tensile properties of *Borassus* fruit fibers, J Appl. Polym. Sci. (2009), 114:603-611(https://doi.org/10.1002/app.30584).

Rinaudo, M., Main properties and current applications of some polysaccharides as biomaterials, Pol. Inter. (2008), 57:397-430(https://doi.org/10.1002/pi.2378).

Saito, T., Kimura, S., Nishiyma, Y., Isogai, A., Cellulose Nanofibers Prepared by TEMPO-Mediated Oxidation of Native Cellulose, Biomac. (2007), 8:2485-2491(https://doi.org/10.1021/bm0703970).

Saito, T., Isogai, A., TEMPO-Mediated Oxidation of Native Cellulose. The Effect of Oxidation Conditions on Chemical and Crystal Structures of the Water-Insoluble Fractions, Biomac. (2004), 5:1983-1989(https://doi.org/10.1021/bm0497769).

Senel, S., Ikinci, G., Kas, S., Yousefi-Rad, A., Sargon, M.F., Hincal, A.A., Chitosan films and hydrogels of chlorhexidine gluconate for oral mucosal delivery, Inter. J. Pharmac. (2000), 193:197-203(https://doi.org/10.1016/S0378-5173(99)00334-8).

Senna, A.M., Botaro, V.R., Biodegradable hydrogel derived from cellulose acetate and EDTA as a reduction substrate of leaching NPK compound fertilizer and water retention in soil, J. Contr. Rel. (2017), 260:194-

201(https://doi.org/10.1016/j.jconrel.2017.06.009).

Senna, A.M., Novack, K.M., Botaro, V.R., Synthesis and characterization of hydrogels from cellulose acetate by esterification crosslinking with EDTA dianhydride, Carbohyd. Pol. (2014), 114:260-268(https://doi.org/10.1016/j.carbpol.2014.08.017).

Siqueira, P., Siqueira, E., de Lima, A., Siqueira, G., Pinzón-Garcia, A., Lopes, A., Segura, M., Isaac, A., Pereira, F., Botaro, V., Three-Dimensional Stable Alginate-Nanocellulose Gels for Biomedical Applications: Towards Tunable Mechanical Properties and Cell Growing, Nanomat. (2019), 9:1-22(https://doi.org/10.3390/nano9010078).

Siqueira, E.J.; and Botaro, V.R., *Luffa cylindrica* fibres/vinylester matrix composites: Effects of 1,2,4,5-benzenetetracarboxylic dianhydride surface modification of the fibres and aluminum hydroxide addition on the properties of the composites, Compos. Sci. Tech. (2013), 82:76-83(https://doi.org/10.1016/j.compscitech.2013.04.012).

Smitha, B., Sridhar, S., Khan, A.A., Chitosan–sodium alginate polyion complexes as fuel cell membranes, Eur. Polym. J. (2005), 41:1859-1866(https://doi.org/10.1016/j.eurpolymj.2005.02.018).

Sun, B., Zhang, M., Hou, Q., Liu, R., Wu, T., Si, C., Further characterization of cellulose nanocrystal (CNC) preparation from sulfuric acid hydrolysis of cotton fibers, Cellulose (2016), 23:439–450(https://doi.org/10.1007/s10570-015-0803-z).

Yang, H., Yan, R., Chen, H., Lee, D.H., Zheng, C., Characteristics of hemicellulose, cellulose and lignin pyrolysis, Fuel (2007), 86:1781-1788(https://doi.org/10.1016/j.fuel.2006.12.013).

Zeng, J., Hu, F., Cheng, Z., Wang, B., Chen, K., Isolation and rheological characterization of cellulose nanofibrils (CNFs) produced by microfluidic homogenization, ball-milling, grinding and refining, Cellulose (2021), 28:3389–3408(https://doi.org/10.1007/s10570-021-03702-3).

Zhou, C., Wu, Q., Yue, Y., Zhang, Q., Application of rod-shaped cellulose nanocrystals in polyacrylamide hydrogels, J. Coll. Int. Sci. (2011), 353:116-123(https://doi.org/10.1016/j.jcis.2010.09.035).

Figures

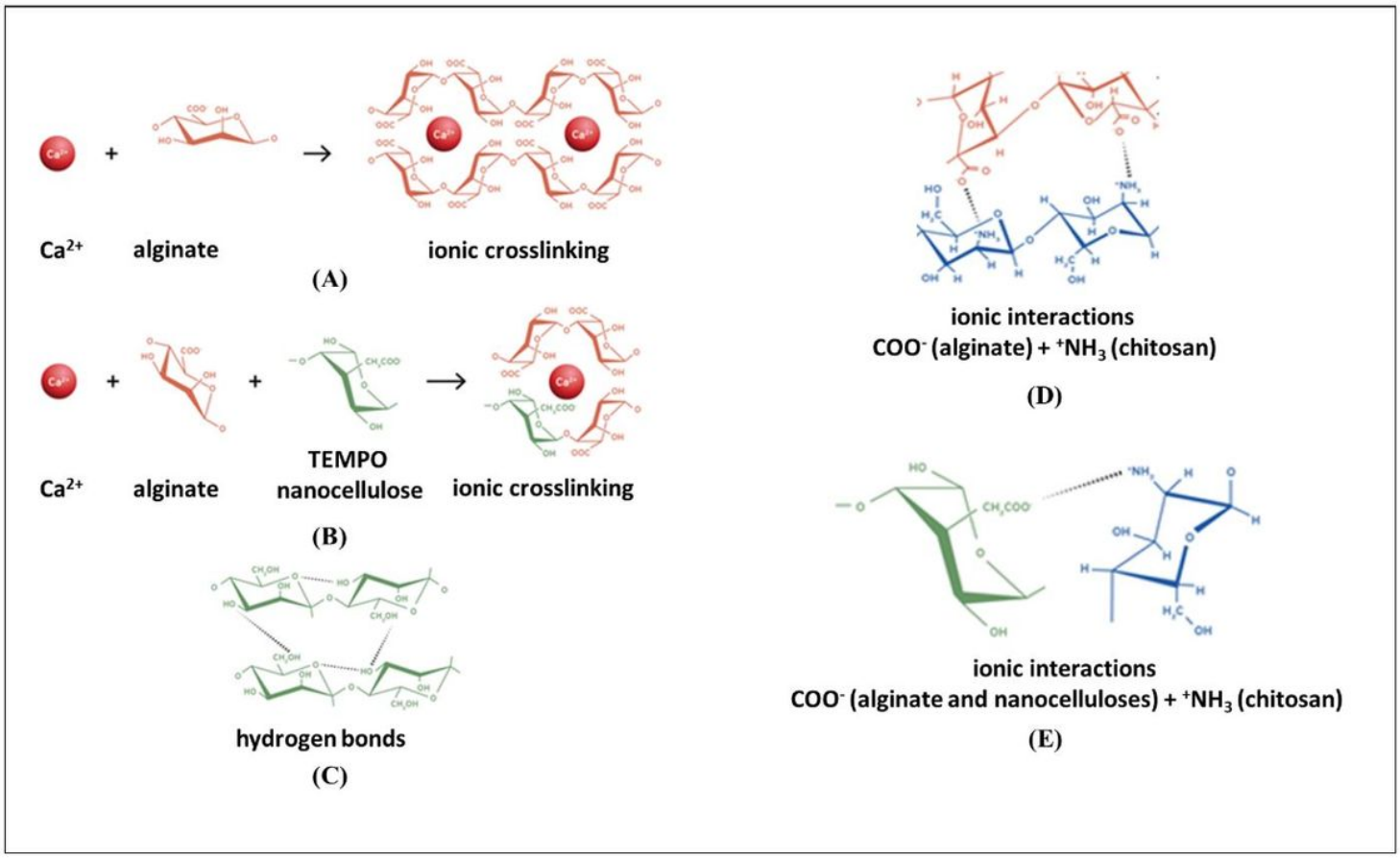

Figure 1

Physicochemical interactions of Alg, Ch and nanocelluloses in the microstructure of the gels: (A) ionic crosslinking of Alg and calcium ions; (B) ionic crosslinking of Alg, TEMPO-oxidized nanocelluloses and calcium ions; (C) secondary interactions of the functional groups of Alg, Ch and nanocelluloses; (D) ionic interactions of Alg and Ch groups; and (E) ionic interactions of negatively charged groups of CNCT's and NFCT's and positively charged groups of Ch chains.

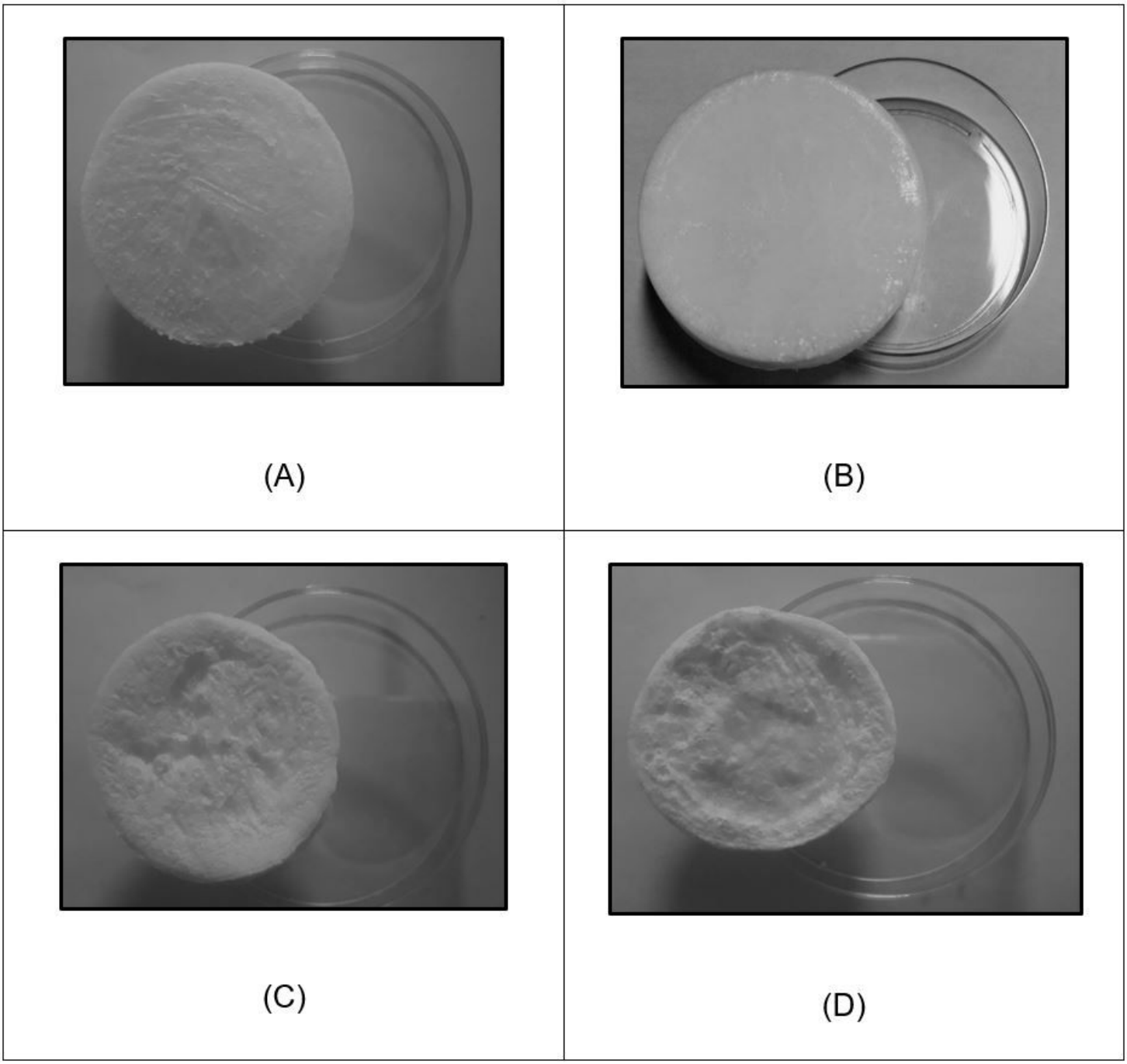

Figure 2

Images of gels after freeze drying: (A) and (B) Alg/Ch/NFCT (at 50 wt%); and (C) and (D) Alg/Ch/CNCT (at 50 wt%).

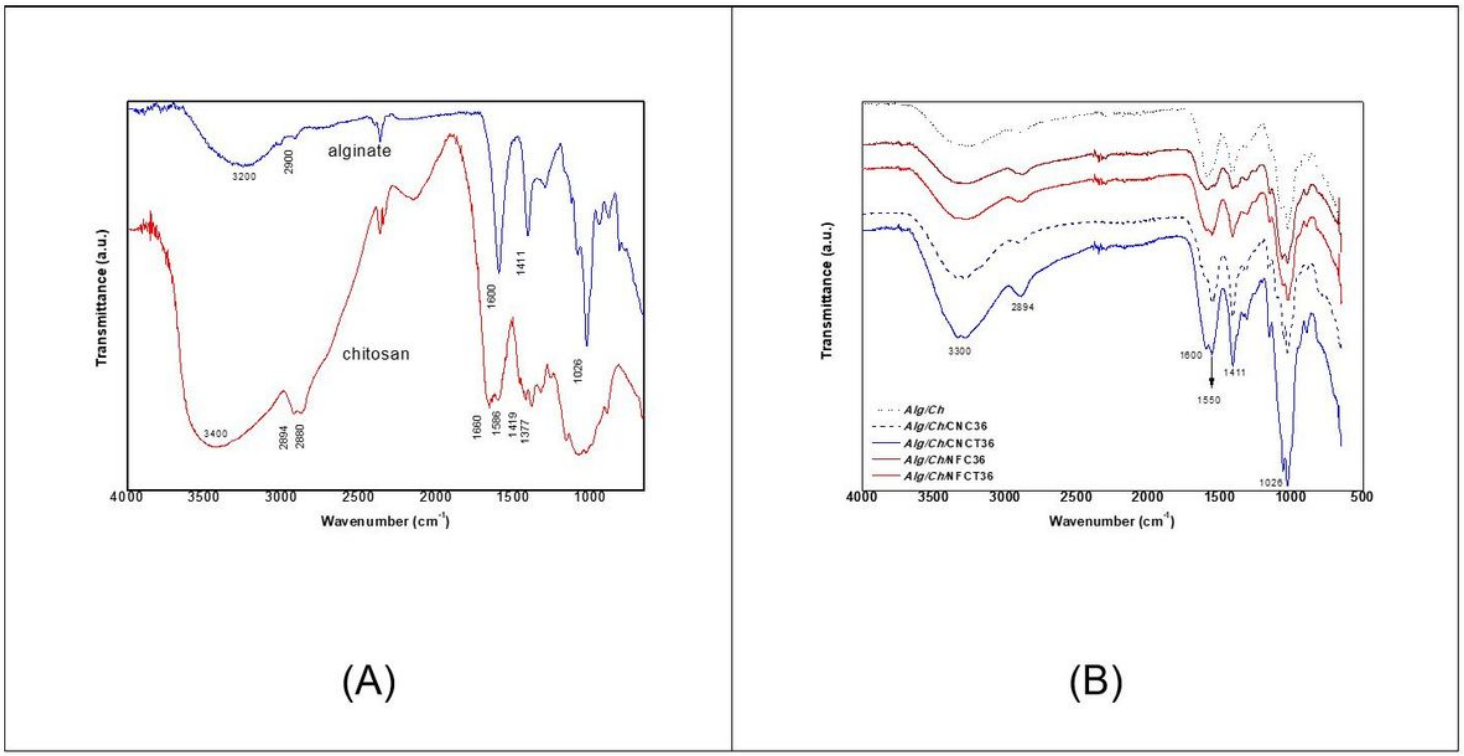

Figure 3

(A) FTIR spectra at ATR mode of Alg and Ch polyelectrolytes and (B) crosslinked Alg/Ch/nanocellulose semi-IPN's.

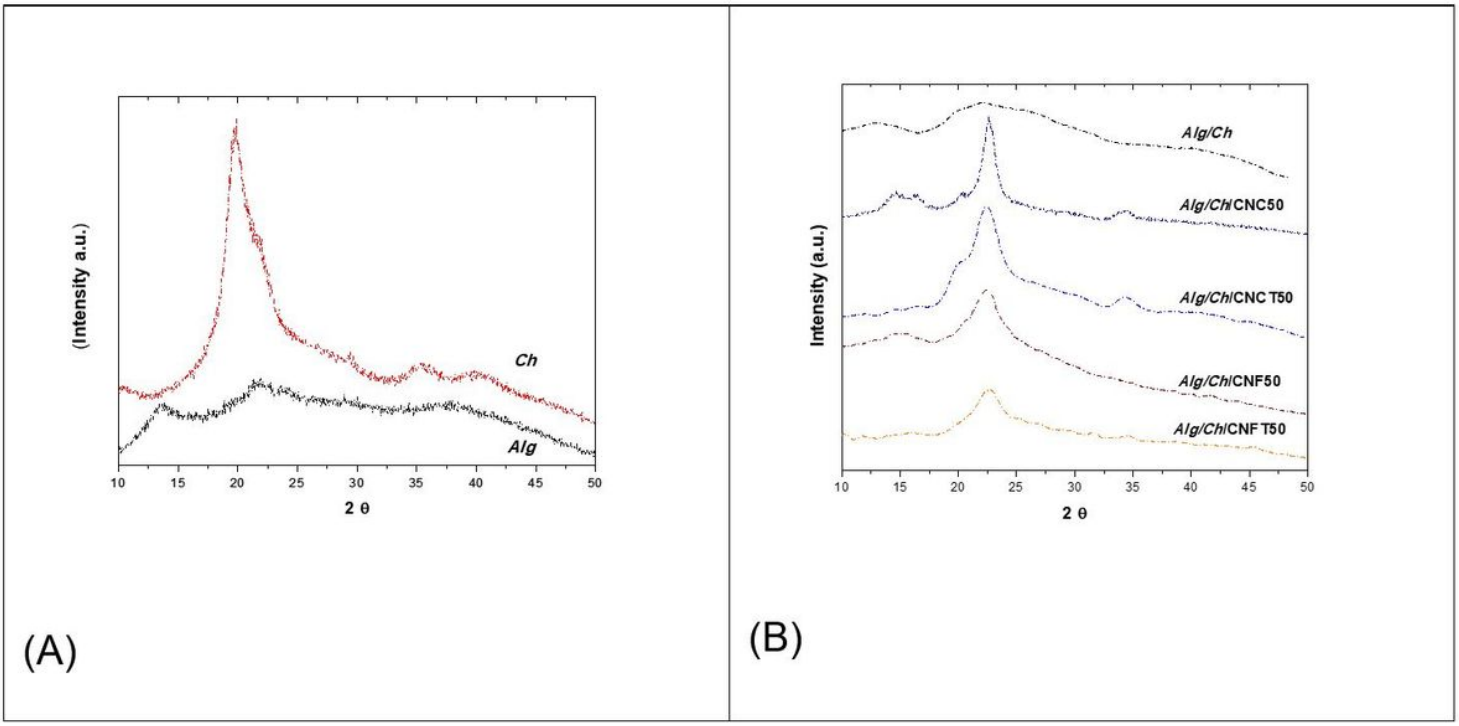

Figure 4

X-ray diffractograms: (A) alginate and chitosan; and (B) crosslinked Alg/Ch/nanocellulose semi-IPN gels.

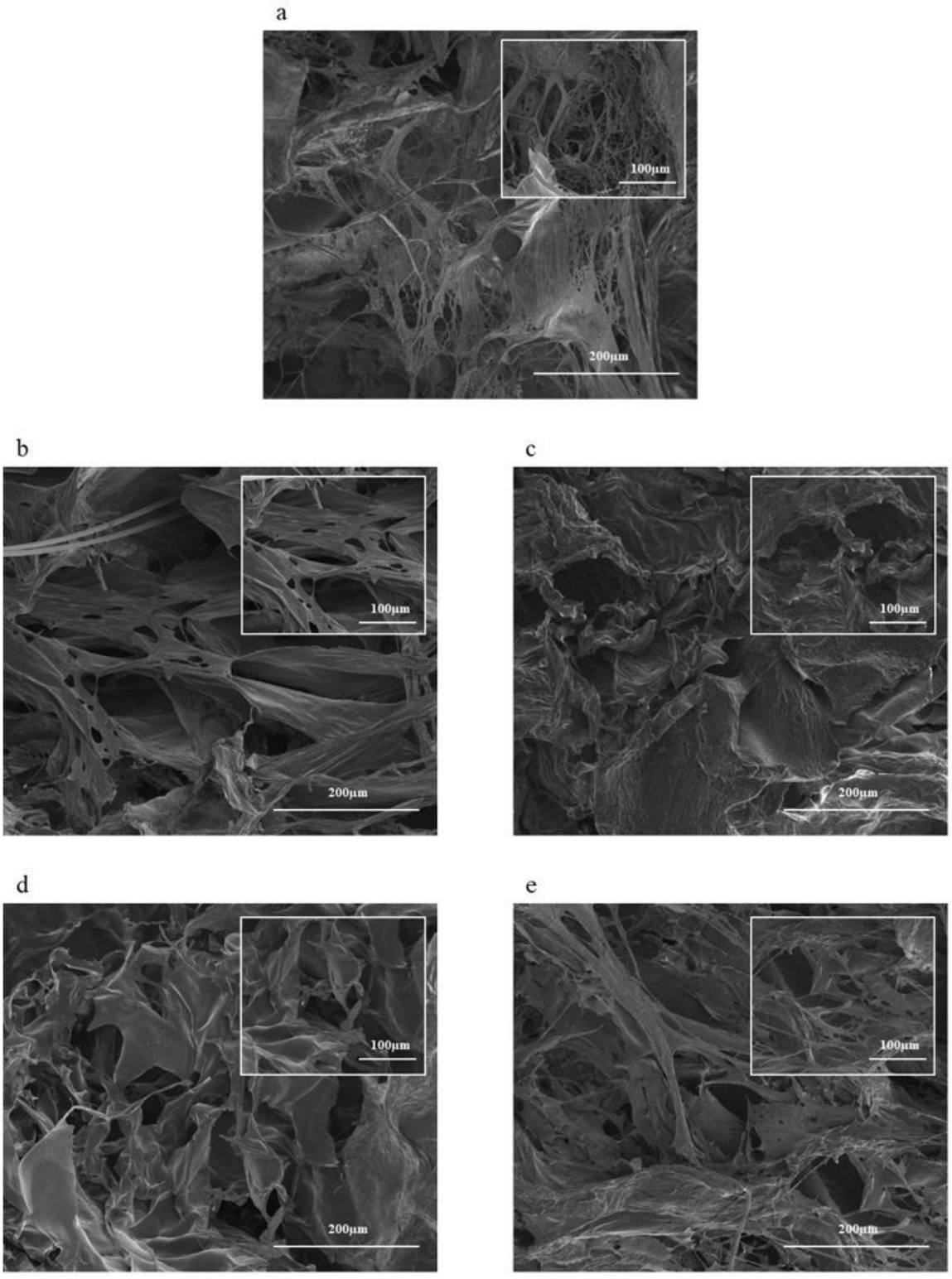

Figure 5

Micrographs obtained by SEM of semi-IPN's at 50 wt% nanocellulose concentration: (A) Alg/Ch semi-IPN's, (B) Alg/Ch/CNC, (C) Alg/Ch/CNCT, (D) Alg/Ch/NFC, (E) Alg/Ch/NFCT (magnification of 500x; the insets represent a magnification of 1000x).

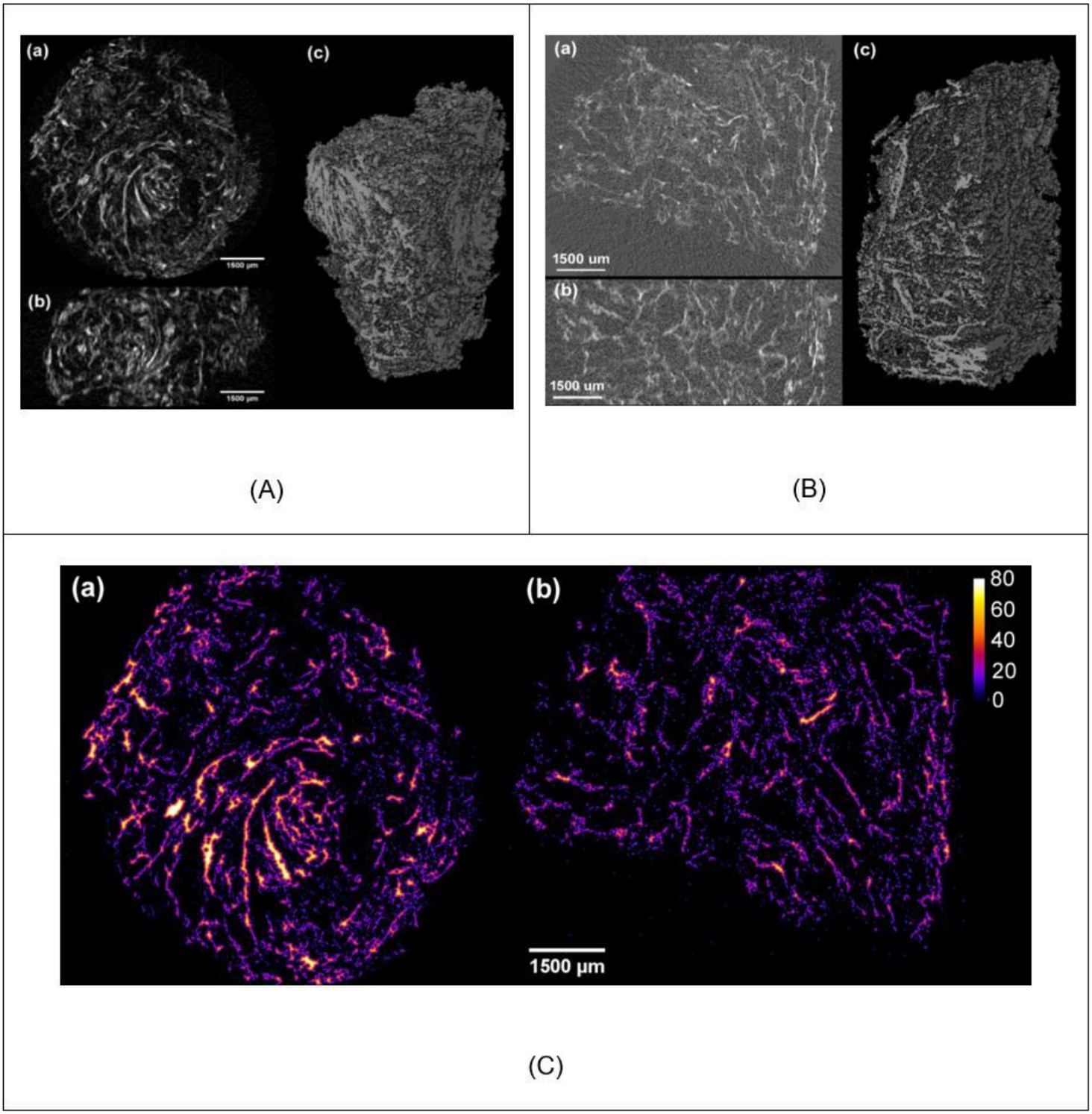

Figure 6

X-ray micro CT images of gels prepared at 50 wt% concentration: (a) Alg/Ch/CNCT semi-IPN's, (b) Alg/Ch/NFCT semi-IPN's, and (C) thickness of pore walls of Alg/Ch/nanocellulose semi-IPN's.

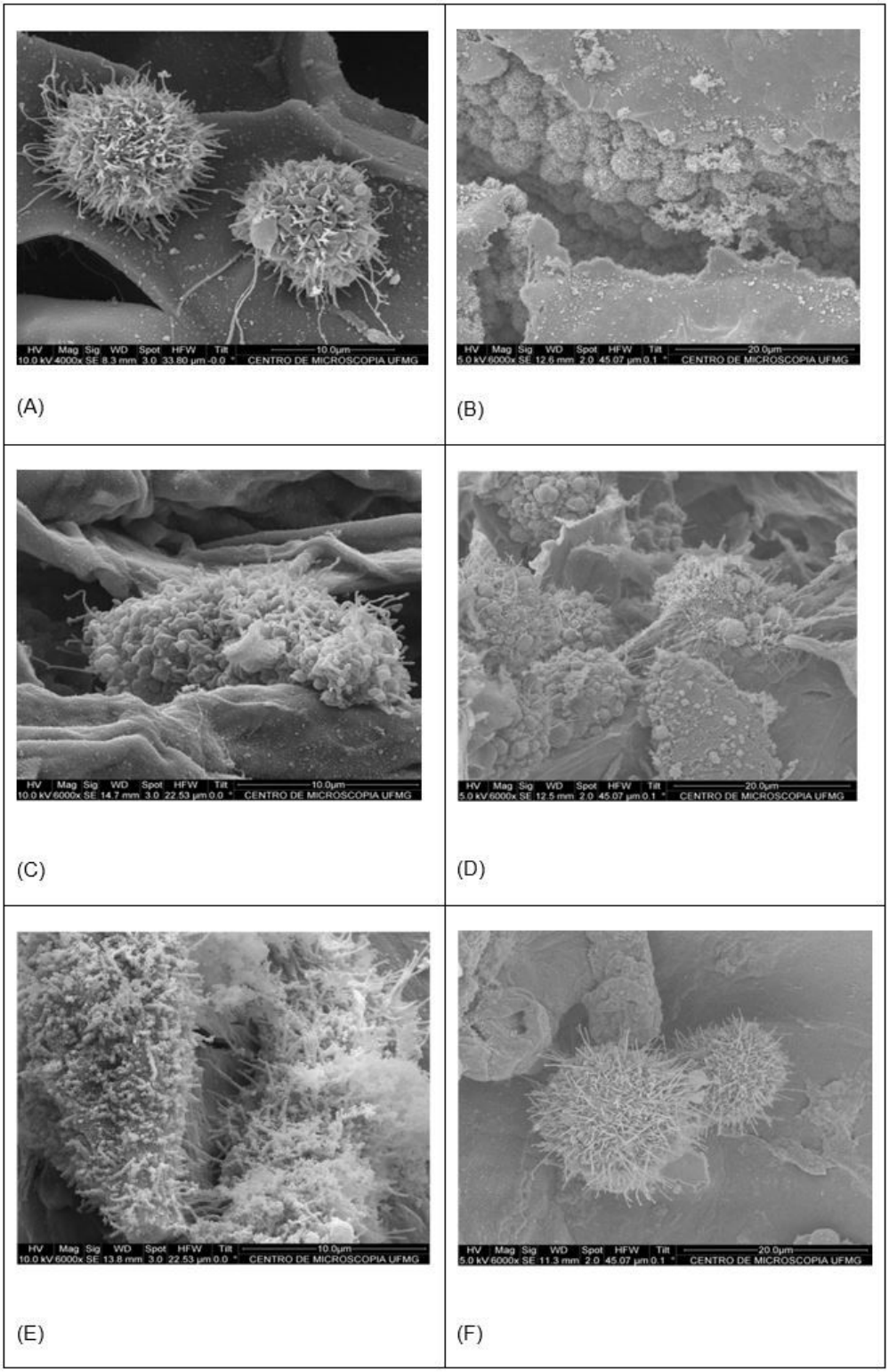

Figure 7

Micrographs obtained by SEM of semi-IPN's: (A) and (B) Alg/Ch, (C) and (D) Alg/Ch/CNCT (at 50 wt%), and (E) and (F) Alg/Ch/NFCT (at 50 wt%).

Supplementary Files

This is a list of supplementary files associated with this preprint. Click to download.

- GraphicalAbstractreviewed.pptx
- SI.docx